

# Virial theorems for vortex states in a confined Bose-Einstein condensate

N. Papanicolaou

*Department of Physics, University of Crete, and Research Center of Crete, Heraklion, Greece*

S. Komineas and N.R. Cooper

*Theory of Condensed Matter Group, Cavendish Laboratory,  
Madingley Road, Cambridge CB3 0HE, United Kingdom*

(Dated: April 23, 2019)

We derive a class of virial theorems which provide stringent tests of both analytical and numerical calculations of vortex states in a confined Bose-Einstein condensate. In the special case of harmonic confinement we arrive at the somewhat surprising conclusion that the linear moments of the particle density, as well as the linear momentum, must vanish even in the presence of off-center vortices which lack axial or reflection symmetry. Illustrations are provided by some analytical results in the limit of a dilute gas, and by a numerical calculation of a class of single and double vortices at intermediate couplings. The effect of anharmonic confinement is also discussed.

PACS numbers: 03.75.Lm, 47.32.Cc, 47.37.+q

Quantized vortices observed in a bulk superfluid such as  $^4\text{He}$  have fascinated physicists for a long time [1] because they provide definite macroscopic manifestations of subtle quantum phenomena. The subject has been significantly enriched in recent years with the realization of ultracold atomic Bose-Einstein condensates (BECs) confined in a finite region, where the strength of effective interactions may be manipulated by varying the number of atoms in a given trap. Typically, these condensates are sufficiently dilute that a mean-field Gross-Pitaevskii (GP) approximation is reliable. It is then possible to explicitly calculate a variety of vortex states which are relevant to experiment. There have been numerous contributions in this area, partly reviewed in Ref. [2], but the subject is still active because a number of finer issues remain unexplored.

The GP approximation is adopted throughout this paper. We mainly consider an effectively two-dimensional (2D) Bose gas of  $N$  atoms, each with mass  $M$ , which interact pairwise with a contact potential of positive strength  $U_0$  and are confined by an axially symmetric external potential  $\hbar\omega_0 V(\rho/a_0)$ . Here the constant  $\omega_0$  carries dimensions of frequency,  $a_0 = \sqrt{\hbar/M\omega_0}$  is the corresponding oscillator length, and  $\rho = \sqrt{x^2 + y^2}$  is the radial distance from the center of the trap. Rationalized units are introduced by measuring time  $t$  in units of  $1/\omega_0$ , distances  $x$  and  $y$  in units of  $a_0$ , while the condensate wave function is rescaled according to  $\Psi \rightarrow \sqrt{N}\Psi/a_0$  and thus acquires unit norm:  $\int \Psi^* \Psi dx dy = 1$ . The energy functional is then given by

$$E = \int \left[ \frac{1}{2} (\nabla \Psi^* \nabla \Psi) + V(\rho) \Psi^* \Psi + \frac{g}{2} (\Psi^* \Psi)^2 \right] dx dy, \quad (1)$$

and yields energy in units of  $\hbar\omega_0 N$ ;  $V(\rho)$  is the rationalized trap potential and  $g = MNU_0/\hbar^2$  is a dimensionless coupling constant.

In a frame rotating about the center of the trap with constant angular frequency  $\omega$  (in units of  $\omega_0$ ) stationary

states of the gas satisfy the time-independent differential equations

$$\begin{aligned} \mu \Psi - i\omega \varepsilon_{\alpha\beta} x_\alpha \partial_\beta \Psi &= \frac{\delta E}{\delta \Psi^*}, \\ \mu \Psi^* + i\omega \varepsilon_{\alpha\beta} x_\alpha \partial_\beta \Psi^* &= \frac{\delta E}{\delta \Psi}, \end{aligned} \quad (2)$$

where

$$\frac{\delta E}{\delta \Psi^*} = -\frac{1}{2} \Delta \Psi + V(\rho) \Psi + g (\Psi^* \Psi) \Psi \quad (3)$$

and  $\delta E/\delta \Psi$  is its complex conjugate. A chemical potential  $\mu$  (in units of  $\hbar\omega_0$ ) is introduced in Eq. (2) in order to enforce a definite number of particles. Greek indices  $\alpha, \beta$  take two distinct values corresponding to the two spatial coordinates  $x_1 = x$  and  $x_2 = y$ , and the Einstein summation convention of the repeated (dummy) indices is consistently employed throughout the paper. Finally,  $\varepsilon_{\alpha\beta}$  is the usual 2D antisymmetric tensor and  $\partial_\alpha = \partial/\partial x_\alpha$ .

Now, given a solution  $\Psi = \Psi(x, y|\mu, \omega)$  of Eqs. (2), the time dependent wave function

$$\begin{aligned} \bar{\Psi}(x, y, t) &= \Psi(x', y'|\mu, \omega) e^{-i\mu t}, \\ x' &= x \cos \omega t + y \sin \omega t, \quad y' = -x \sin \omega t + y \cos \omega t, \end{aligned} \quad (4)$$

satisfies the standard Gross-Pitaevskii equation in the laboratory frame ( $i \partial \bar{\Psi}/\partial t = \delta E/\delta \bar{\Psi}^*$ ) and may be thought of as a configuration that rotates (precesses) about the center of the trap with angular frequency  $\omega$ . While all calculations will be based on the stationary Eqs. (2), Eq. (4) is important for a proper interpretation of the results.

Before discussing explicit solutions, we derive a class of virial theorems which follow directly from Eqs. (2). Thus we multiply both sides of the first equation by  $\Psi^*$ , the second by  $\Psi$ , and add the two equations. We then integrate both sides over the entire  $xy$  plane and apply partial integration to obtain

$$\mu + \omega \ell = E_{\text{kin}} + E_{\text{trap}} + 2E_{\text{pot}}, \quad (5)$$

where  $E_{\text{kin}}$ ,  $E_{\text{trap}}$  and  $E_{\text{pot}}$  correspond to the three terms in the total energy  $E$  of Eq. (1). In the left hand side of Eq. (5) we have employed the relations

$$\int \Psi^* \Psi \, dx dy = 1, \quad \ell = \frac{1}{i} \int \Psi^* \varepsilon_{\alpha\beta} x_\alpha \partial_\beta \Psi \, dx dy, \quad (6)$$

where the first is consistent with our choice of rationalized units and the second is the definition of the angular momentum per particle (in units of  $\hbar$ ). Eq. (5) is the first of a series of virial relations that must be satisfied by all solutions of Eqs. (2).

We now repeat the procedure by multiplying the first Eq. (2) by  $\Psi^*$ , the second by  $\Psi$ , and then subtracting the two equations to obtain

$$\begin{aligned} -\omega \varepsilon_{\alpha\beta} x_\alpha \partial_\beta n + \partial_\alpha J_\alpha &= 0, \\ n = \Psi^* \Psi, \quad J_\alpha &= \frac{1}{2i} (\Psi^* \partial_\alpha \Psi - \Psi \partial_\alpha \Psi^*), \end{aligned} \quad (7)$$

where  $n$  and  $\mathbf{J}$  are the familiar particle and current densities. The same result could be derived by applying the continuity equation in the laboratory frame ( $\partial n / \partial t + \nabla \cdot \mathbf{J} = 0$ ) for a wave function of the form (4). Now multiply both sides of Eq. (7) by  $x_\alpha$  and then apply partial integration to obtain the virial relation

$$\begin{aligned} P_\alpha + \omega \varepsilon_{\alpha\beta} R_\beta &= 0, \\ P_\alpha &\equiv \int J_\alpha \, dx dy, \quad R_\alpha \equiv \int x_\alpha n \, dx dy, \end{aligned} \quad (8)$$

where  $\mathbf{P} = (P_1, P_2)$  is the linear momentum in the rotating frame and  $\mathbf{R} = (R_1, R_2)$  may be thought of as the mean position of the configuration in question. It should be clear that neither  $\mathbf{P}$  nor  $\mathbf{R}$  is conserved in the laboratory frame, where they precess about the center with frequency  $\omega$ , in complete analogy with the momentum and position of a pointlike particle in circular motion. In view of this analogy the virial relation (8) appears to be quite natural.

A third and more elaborate class of virial relations is obtained starting again from Eqs. (2) but now multiply the first equation by  $\partial_\alpha \Psi^*$ , the second by  $\partial_\alpha \Psi$ , and then add the two equations to yield after some rearrangement

$$\mu \partial_\alpha n + \omega x_\alpha \gamma = \frac{\delta E}{\delta \Psi^*} \partial_\alpha \Psi^* + \frac{\delta E}{\delta \Psi} \partial_\alpha \Psi \equiv f_\alpha \quad (9)$$

where  $n = \Psi^* \Psi$  is again the particle density,

$$\gamma = \frac{1}{i} \varepsilon_{\alpha\beta} \partial_\alpha \Psi^* \partial_\beta \Psi \quad (10)$$

may be referred to as the topological vorticity [3, 4, 5], and we further use Eq. (3) to write

$$\begin{aligned} f_\alpha &= \partial_\beta \sigma_{\alpha\beta} + V(\rho) \partial_\alpha n, \\ \sigma_{\alpha\beta} &= w \delta_{\alpha\beta} - \frac{1}{2} (\partial_\alpha \Psi^* \partial_\beta \Psi + \partial_\beta \Psi^* \partial_\alpha \Psi), \\ w &= \frac{1}{2} [(\nabla \Psi^* \cdot \nabla \Psi) + g(\Psi^* \Psi)^2]. \end{aligned} \quad (11)$$

Hence Eq. (9) reduces to a more transparent form:

$$\mu \partial_\alpha n + \omega x_\alpha \gamma = \partial_\beta \sigma_{\alpha\beta} + V(\rho) \partial_\alpha n, \quad (12)$$

which will provide the basis for the derivation of a number of interesting virial relations.

Some key elements of the preceding discussion, such as the topological vorticity  $\gamma$  and the tensor  $\sigma_{\alpha\beta}$ , appeared earlier in a study of the magnetic continuum [3, 5] as well as of homogeneous superfluids [4]. In the latter case, the total topological vorticity  $\Gamma = \int \gamma \, dx dy = 2\pi n$  is integer valued ( $n = 0, \pm 1, \pm 2, \dots$ ) for wave functions that satisfy the boundary condition  $|\Psi| \rightarrow 1$  at spatial infinity. However, for the confined gas under present consideration, the relevant wave functions satisfy the boundary condition  $|\Psi| \rightarrow 0$  which leads to  $\Gamma = 0$  by a straightforward partial integration. Similarly, the linear and angular momenta defined from

$$P_\alpha = \int \varepsilon_{\alpha\beta} x_\beta \gamma \, dx dy, \quad \ell = -\frac{1}{2} \int \rho^2 \gamma \, dx dy, \quad (13)$$

may be shown to coincide with the standard definitions given in Eqs. (6) and (8) by freely performing partial integrations which are fully justified in a confined gas. In contrast, partial integrations are generally ambiguous in a homogeneous gas and Eqs. (13) do not coincide with the standard definitions, thus leading to a subtle distinction between momentum and impulse [6, 7]. Certainly, for our current purposes, Eqs. (13) may be employed in conjunction with Eq. (12) without further questioning.

Thus we integrate both sides of Eq. (12) over the entire  $xy$  plane and note that the terms  $\partial_\alpha n$  and  $\partial_\beta \sigma_{\alpha\beta}$  lead to vanishing surface integrals at spatial infinity. The remaining terms may be arranged to yield the virial relation

$$\omega P_\alpha + \varepsilon_{\alpha\beta} \int \frac{x_\beta}{\rho} V' n \, dx dy = 0, \quad (14)$$

where we have employed the linear momentum  $P_\alpha$  from Eq. (13) and performed a partial integration in the second term, with  $V' = dV/d\rho$ .

The basic relation (12) may be further iterated by multiplying both sides with  $x_\beta$  and then integrating over all space to obtain

$$\begin{aligned} \mu \delta_{\alpha\beta} - \omega \int x_\alpha x_\beta \gamma \, dx dy = \\ \int \sigma_{\alpha\beta} \, dx dy + \int \left( V \delta_{\alpha\beta} + \frac{x_\alpha x_\beta}{\rho} V' \right) n \, dx dy, \end{aligned} \quad (15)$$

which may be applied for any combination of indices  $\alpha$  and  $\beta$  and thus contains three independent virial relations. An interesting special case is obtained by taking the trace of both sides of Eq. (15):

$$\begin{aligned} 2\mu - \omega \int \rho^2 \gamma \, dx dy = \\ \int \text{tr} \sigma \, dx dy + \int (2V + \rho V') n \, dx dy, \end{aligned} \quad (16)$$

where we may further insert the definition of the angular momentum  $\ell$  from Eq. (13) and  $tr\sigma = g(\Psi^*\Psi)^2$  from Eq. (11) to write

$$\mu + \omega\ell = E_{\text{pot}} + \int (V + \frac{1}{2}\rho V') n dx dy. \quad (17)$$

This virial relation may be derived also by applying a Derrick-like [8] scaling argument to the extended energy functional  $F = E - \omega L - \mu N$ .

Eqs. (5), (8), (14) and (17) already provide an interesting variety of virial theorems which are employed in the following to check and analyze explicit solutions of Eqs. (2). It should be noted that virial relations (5) and (8) are insensitive to the specific choice of the trap potential, while (14) and (17) depend crucially on the choice of  $V = V(\rho)$ . Similarly, Eqs. (8) and (14) are insensitive to the specific form of the tensor  $\sigma_{\alpha\beta}$  and are thus valid for any type of interparticle interactions.

Most of the theoretical models employed to describe realistic BECs assume a harmonic trap potential  $V = \frac{1}{2}\rho^2$  and, hence,  $V' = \rho$ . The virial relation (17) may then be written in the form  $\mu + \omega\ell = E_{\text{pot}} + 2E_{\text{trap}}$  which is combined with Eq. (5) to yield

$$E_{\text{kin}} + E_{\text{pot}} = E_{\text{trap}}. \quad (18)$$

This relation does not contradict the existence of finite-energy stationary solutions in the rotating frame and must indeed be verified by any such solution of Eqs. (2). Similarly, the virial relation (14) simplifies for  $V' = \rho$  to read  $\omega P_\alpha + \varepsilon_{\alpha\beta} R_\beta = 0$  which may be combined with Eq. (8) to arrive at the somewhat surprising conclusion that both the linear momentum and the linear moments of the particle density must vanish in a harmonic trap:

$$P_\alpha = 0 = R_\alpha, \quad (19)$$

provided that  $\omega \neq 1$ , a restriction that is not essential in the case of repulsive interactions because stationary states are then possible in a harmonic trap only for  $\omega < 1 (= \omega_0)$ . In the special limit  $\omega = 1$ , which could be achieved in the case of attractive interactions [9],  $P$  and  $R$  need not vanish.

A simple explanation of the preceding result can be obtained by noting that for a system of atoms in a harmonic trap with translationally-invariant interparticle interactions, the center-of-mass (CM) coordinate separates from the internal coordinates and behaves as a free particle in a harmonic well. For  $\omega < 1$ , the CM must be in its ground state, so  $P$  and  $R$  must be zero because they depend only on the CM coordinates. At  $\omega = 1$ , it is possible to put the CM into a rotating state with nonzero  $P$  and  $R$ . This is relevant for the case of attractive interactions where the rotating states with  $\omega = 1$  are such that the angular momentum is carried by the center-of-mass [9]. This viewpoint makes it clear that the same result will apply for any translationally invariant interparticle interactions, in the case of 3D harmonic confinement, and beyond the GP approximation (for the

expectation value of the CM and conjugate momentum). It is also clear that Eq. (19) is not valid in the case of anharmonic confinement, as discussed later in this paper.

Explicit solutions of the Gross-Pitaevskii theory were initially obtained in the limit of a very dilute gas [10]. A wave function with definite angular momentum  $\ell$  may then be restricted to the lowest Landau level (LLL):

$$\Psi = \sum_{m \geq 0} c_m \Psi_m, \quad \Psi_m = \frac{z^m e^{-|z|^2/2}}{\sqrt{m! \pi}}, \quad (20)$$

where the sum extends over nonnegative integer  $m$  (for positive  $\ell$ ) and  $z = x + iy$ . The unknown coefficients  $c_m$  are calculated by minimizing the total energy  $E = \ell + g/2 \int (\Psi^* \Psi)^2 dx dy$  under the constraints  $\sum |c_m|^2 = 1$  and  $\sum m |c_m|^2 = \ell$ . This task was initially [10] carried out numerically to furnish an impressive variety of vortex states leading up to a vortex lattice for large  $\ell$ . For small  $\ell$ , some analytical results were obtained [11] by a perturbative expansion of the coefficients  $c_m$  in powers of  $\ell$  or  $\bar{\ell} = 1 - \ell$ .

These results may already be used to illustrate the virial relations (19). We first consider the linear moments of the particle density  $R_\alpha$ , with  $\alpha = 1$  or  $2$ , or their complex combination  $R_1 + iR_2 = \int \Psi^* z \Psi dx dy$ . We may then insert the series representation (20) for the wave function  $\Psi$ , note that  $z \Psi_m = \sqrt{m+1} \Psi_{m+1}$ , and apply the usual orthogonality relations for the  $\Psi_m$ 's to obtain

$$R_1 + iR_2 = \sum_{m \geq 0} \sqrt{m+1} c_{m+1}^* c_m. \quad (21)$$

If we now use the perturbative expansions for the  $c_m$ 's from Ref. [11], with due attention to phase (sign) conventions [12], we find that  $R_1 + iR_2 = 0$  order-by-order in a consistent expansion in powers of  $\ell$  or  $\bar{\ell} = 1 - \ell$ . A similar calculation of the linear momentum yields  $P_1 + iP_2 = 0$ , thus confirming the validity of both virial relations in Eq. (19), as well as providing a nontrivial check of consistency of the results of Ref. [11].

A more convincing demonstration is possible over the entire range  $0 < \ell < 1$  where a closed-form expression for the optimal LLL wave function was recently achieved [13]:

$$\Psi = \frac{\ell^{\frac{1}{4}}}{\sqrt{\pi}} [(x-b) + iy] e^{-\frac{1}{2}[(x-a)^2 - 2ia y + y^2]} \\ a = (\sqrt{\bar{\ell}} - \ell)^{1/2}, \quad b = \frac{1-\ell}{a}, \quad (22)$$

which describes an off-center vortex located on the  $x$  axis, modulo an overall azimuthal rotation, at a distance  $b = b(\ell)$  from the center of the trap. For  $\ell \rightarrow 0$  ( $b \rightarrow \infty$ ) the vortex is expelled from the system, while for  $\ell \rightarrow 1$  ( $b \rightarrow 0$ ) the vortex moves to the center and becomes axially symmetric. The corresponding particle density reads

$$n = \frac{\sqrt{\bar{\ell}}}{\pi} [(x-b)^2 + y^2] e^{-(x-a)^2 - y^2} \quad (23)$$

and lacks axial or reflection symmetry except for  $\ell = 0$  or 1. Nevertheless, an explicit calculation shows that

$$R_1 = \int x n dx dy = \sqrt{\ell} [2a - b + a(a - b)^2] = 0, \quad (24)$$

using the explicit expressions for  $a$  and  $b$  from Eq. (22), and  $R_2 = \int y n dx dy = 0$ , thanks to the  $y \rightarrow -y$  symmetry of the particle density. A similar calculation shows that the linear momentum  $\mathbf{P} = (P_1, P_2)$  also vanishes, thus verifying both virial relations in Eq. (19) in spite of the lack of axial or reflection symmetry in the wave function (22). This result appears to be surprising if we naively view the off-center vortex as a pointlike particle rotating on a circle with radius  $b$ . In fact, the spatial distribution of particle and current densities is more subtle in an off-center vortex and leads to vanishing  $\mathbf{P}$  and  $\mathbf{R}$ , even though the vortex does precess about the center of the trap. As we shall see shortly, this curious result is valid only for harmonic confinement ( $V = \frac{1}{2}\rho^2$ ).

We complete the discussion of the dilute-gas limit by quoting the energy  $E$  and frequency  $\omega$  associated with the wave function (22):

$$E = \ell + \frac{g}{4\pi} \left(1 - \frac{\ell}{2}\right), \quad \omega = \frac{dE}{d\ell} = 1 - \delta, \quad (25)$$

with  $\delta \equiv g/8\pi$ , a result that is valid in the limit  $\delta \ll 1$ . A notable feature of this limit is that frequency  $\omega$  is independent of angular momentum  $\ell$  [9, 10, 11, 13].

One should keep in mind that practically all experiments have been performed on BECs with  $\delta > 1$ , often  $\delta \gg 1$ , where the weak coupling (LLL) theory is no longer valid. A numerical solution of Eqs. (2) is necessary for strong couplings. A numerical method developed in [14] is based on a norm-preserving relaxation algorithm which, in effect, capitalizes on the virial relation (5) to find a wave function of unit norm that is a (local) minimum of the energy functional in the rotating frame:  $E_{\text{rot}} = E - \omega\ell$ . Here we employ a variation of the norm-preserving algorithm to minimize instead the Lyapunov functional  $E' = E + \frac{1}{2}a(\ell - b)^2$  where  $a$  and  $b$  are arbitrary constants with  $a > 0$ . Local minima of  $E'$  satisfy Eqs. (2) with frequency determined self-consistently from  $\omega = a(b - \ell)$  and chemical potential  $\mu$  from Eq. (5). The constants  $a$  and  $b$  are chosen (tuned) to ensure convergence to nontrivial solutions with angular momentum  $\ell$  in the desired range. The advantage of this algorithm is that it finds solutions of Eqs. (2) which are stationary points but not necessarily local minima of the functional  $E_{\text{rot}}$ .

In the following we describe a class of solutions for the intermediate coupling  $\delta = g/8\pi = 2$  where the LLL approximation is quantitatively inaccurate. Needless to say, all virial relations, including Eqs. (18) and (19) were confirmed by our solutions to within numerical accuracy. In Fig. 1 we present contour plots of the particle density  $n$  for four characteristic values of angular momentum in the range  $0 < \ell < 2$ , whereas Fig. 2 shows the results for

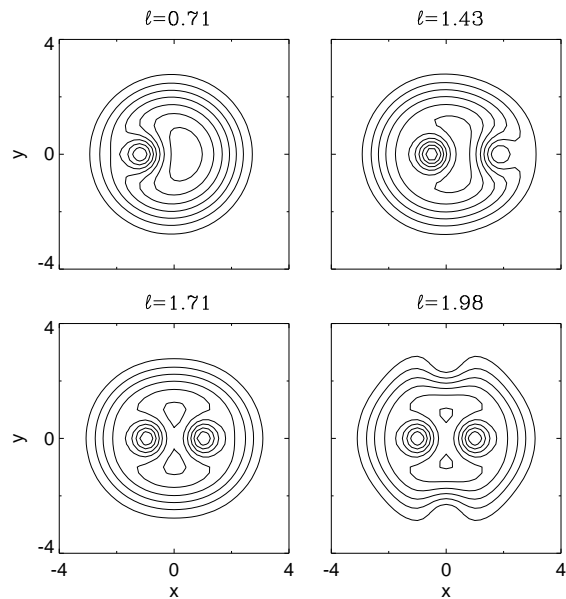


FIG. 1: Contour plots of the particle density  $n$  for a class of vortex states calculated in a harmonic trap with  $\delta = 2$ . The four characteristic values of the angular momentum  $\ell$  correspond to the four branches  $AB$ ,  $B'\Gamma$ ,  $\Gamma\Delta$ , and  $\Delta\dots$  in Fig. 2.

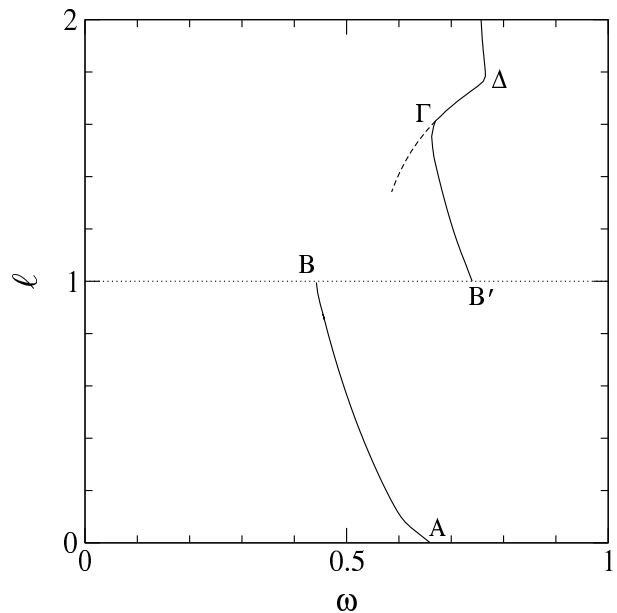


FIG. 2: Angular frequency  $\omega$  (in units of  $\omega_0$ ) as a function of angular momentum per particle  $\ell$  (in units of  $\hbar$ ) for a class of vortex states calculated in a harmonic trap with  $\delta = 2$ .

the frequency dispersion  $\omega = dE/d\ell = \omega(\ell)$  throughout the same range.

For  $0 < \ell < 1$  the calculated configuration is an off-center vortex with energy  $E(\ell)$  that is a concave function of  $\ell$ . Thus the frequency  $\omega = dE/d\ell$  is a decreasing function of angular momentum taking values in the fi-

nite range  $\omega_B < \omega < \omega_A$  with  $\omega_B = 0.44$  for  $\ell \rightarrow 1^-$  and  $\omega_A = 0.62$  for  $\ell \rightarrow 0$ . The vortex precesses faster the farther it is located from the center of the trap ( $\ell \rightarrow 0$ ). In the opposite limit ( $\ell \rightarrow 1^-$ ) the vortex moves to the center and becomes axially symmetric. There is no sense of precession in such a vortex because the limiting frequency  $\omega_B$  may then be absorbed into an effective chemical potential  $\bar{\mu} = \mu + \omega_B$  and the wave function (4) reduces to a quasi-static configuration with chemical potential  $\bar{\mu}$ . Also note that the band of allowed frequencies reduces to a single point  $\omega_A = \omega_B = 1 - \delta$  in the dilute-gas limit ( $\delta \ll 1$ ), as is evident from Eq. (25).

As the angular momentum increases beyond unity the energy remains continuous, but its first derivative exhibits a finite jump which leads to a new limiting frequency  $\omega_{B'} = 0.74$  for  $\ell \rightarrow 1^+$ . The original vortex becomes again displaced from the center for  $\ell = 1^+$  and a second off-center vortex appears at an asymmetric position on the opposite side of the trap. This picture remains largely correct in the region  $1 < \ell < 1.55$  and leads to branch  $B'\Gamma$  in Fig. 2 with limiting frequencies  $\omega_{B'} = 0.74$  and  $\omega_\Gamma = 0.66$ . Energy is again concave in this region and thus frequency is a decreasing function of angular momentum.

At point  $\Gamma$  ( $\ell = 1.55$ ) the calculated configuration becomes a reflection-symmetric two-vortex state where the two vortices are located at the same distance on opposite sides from the center of the trap. Such a symmetric state persists throughout the branch  $\Gamma\Delta$  ( $1.55 < \ell < 1.78$ ) with corresponding frequencies in the range  $0.66 < \omega < 0.76$ . Incidentally,  $\Gamma\Delta$  is the only branch where the energy  $E(\ell)$  is convex and thus the frequency  $\omega(\ell)$  is an increasing function of angular momentum.

Beyond point  $\Delta$  ( $\ell > 1.78$ ) the frequency becomes once again a decreasing function of angular momentum. This region seems to be characterized by the appearance of a new pair of vortices symmetrically displayed along the  $y$  axis, as indicated by the fourth ( $\ell=1.98$ ) entry of Fig. 1. Nevertheless, reflection symmetry appears to persist in this region. A related interesting question is whether or not hysteresis sets in when we reverse the cycle by reducing the angular momentum from, say,  $\ell = 1.98$ . While the cycle is perfectly reproduced down to point  $\Gamma$ , a reflection symmetric two-vortex state persists for some range of angular momenta below  $\ell_\Gamma = 1.55$ , as indicated by the dashed line in Fig. 2.

The issue of stability of the calculated vortex states is rather delicate and may well depend on the specific experimental protocol. According to [10] mechanical stability requires that the energy be a convex function of angular momentum:  $d\omega/d\ell = d^2E/d\ell^2 > 0$ . This condition is satisfied only by the  $\Gamma\Delta$  branch of Fig. 2 which corresponds to symmetric two-vortex states. In particular, the whole of the AB branch, which corresponds to single off-center vortices, does not satisfy the criterion of mechanical stability. Nevertheless, precessing off-center vortices have been observed experimentally in a spherical trap [15]. Although the current two-dimensional cal-

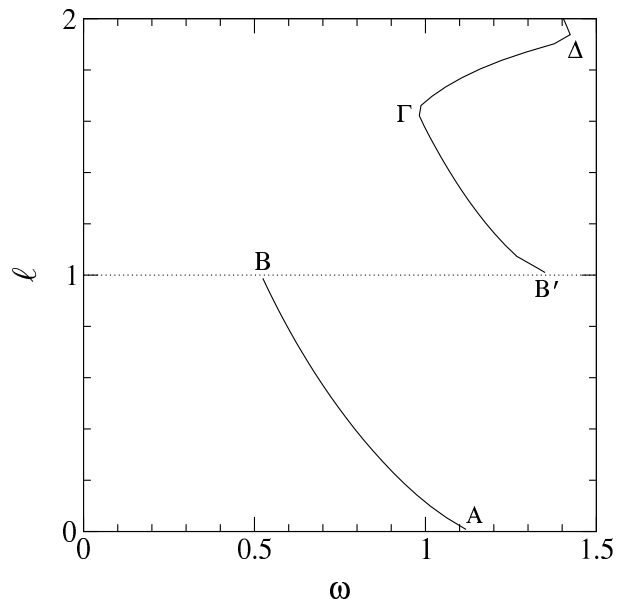


FIG. 3: Angular frequency  $\omega$  as a function of angular momentum per particle  $\ell$  for a class of vortex states calculated in an anharmonic trap with  $\delta = 2$  and  $\lambda = 1/4$ .

ulation does not directly apply to a spherical trap, a similar three-dimensional calculation [16] leads to a class of U-shaped off-center vortices whose frequency dispersion is completely analogous to the AB branch of Fig. 2. Furthermore, the frequencies of precession measured in the experiment lie within the calculated frequency band  $[\omega_B, \omega_A]$ . To conclude this digression, we note that the virial relations (19) are valid also in a three-dimensional axially symmetric harmonic trap, with  $\alpha = 1$  or  $2$  corresponding to the directions perpendicular to the symmetry (rotation) axis, to be completed with  $P_3 = 0 = R_3$  along the same axis.

Finally, we consider the effect of anharmonic confinement modelled here by the rationalized trap potential

$$V = \frac{1}{2} \rho^2 (1 + \lambda \rho^2), \quad V' = \rho + 2\lambda \rho^3, \quad (26)$$

which is thought to describe the trap used in the experiment of Ref. [17] with  $\lambda \sim 10^{-3}$ . In our numerical calculation we adopted a much larger  $\lambda$  in order to emphasize some generic features of anharmonicity. We have thus repeated our earlier calculation of vortex states in a harmonic trap ( $\lambda = 0$ ) now for  $\lambda = 1/4$  but the same coupling constant  $\delta = g/8\pi = 2$ .

The calculated frequency dispersion is shown in Fig. 3 which differs from Fig. 2 mainly by the fact that the dispersion now extends well beyond  $\omega = 1 (= \omega_0)$  because the condition  $\omega < 1$  is no longer necessary to ensure stability of the rotating gas. At first sight, the vortex configurations that correspond to the various branches of Fig. 3 are also similar to those calculated for the harmonic trap and shown in Fig. 1. However, a closer look reveals some subtle differences which are best illustrated

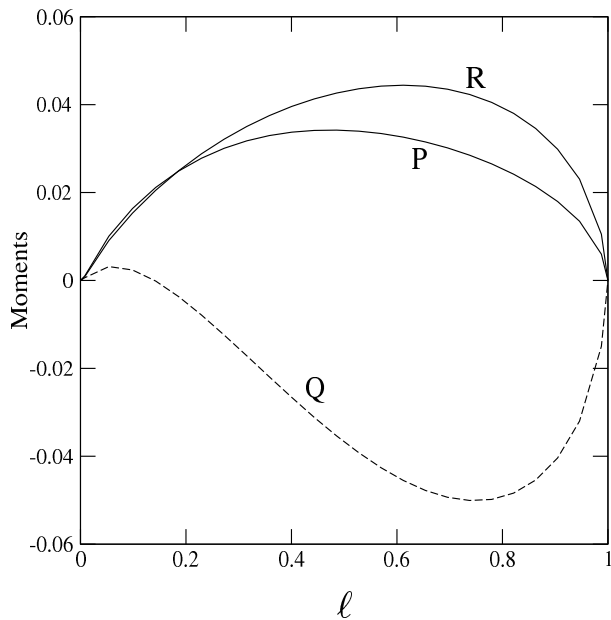


FIG. 4: Linear momentum  $P$  (in units of  $\hbar/a_0$ ), linear moment  $R$  (in units of  $a_0$ ), and generalized moment  $Q$  (in units of  $a_0^3$ ), as functions of angular momentum per particle  $\ell$  (in units of  $\hbar$ ), for single off-center vortices in an anharmonic trap with  $\delta = 2$  and  $\lambda = 1/4$ .

by recalling the virial relation (14) now applied for the potential  $V$  of Eq. (26):

$$\begin{aligned} \omega P_\alpha + \varepsilon_{\alpha\beta} R_\beta &= -2\lambda \varepsilon_{\alpha\beta} Q_\beta, \\ Q_\alpha &\equiv \int x_\alpha \rho^2 n \, dx dy, \end{aligned} \quad (27)$$

where  $Q_\alpha$  is a generalized (higher) moment of the particle density. We further recall virial relation (8), which is valid for any trap potential, and combine it with Eq. (27) to yield

$$P_\alpha = \frac{2\lambda\omega}{1-\omega^2} \varepsilon_{\alpha\beta} Q_\beta, \quad R_\alpha = -\frac{2\lambda}{1-\omega^2} Q_\alpha, \quad (28)$$

which differ significantly from Eqs. (19) in that the linear momentum  $\mathbf{P}$  and moment  $\mathbf{R}$  are no longer forced to vanish.

For a numerical illustration we consider the class of single off-center vortices, which correspond to the AB

branch of Fig. 3, and assume without loss of generality that the vortex is located on the  $x$  axis. We may then insert  $\mathbf{P} = (0, P)$ ,  $\mathbf{R} = (R, 0)$  and  $\mathbf{Q} = (Q, 0)$  in Eqs. (28) to obtain the more transparent relations

$$P = -\frac{2\lambda\omega}{1-\omega^2} Q, \quad R = -\frac{2\lambda}{1-\omega^2} Q. \quad (29)$$

The moments  $P$ ,  $R$  and  $Q$  calculated along the AB branch ( $0 < \ell < 1$ ) were found to satisfy the virial relations (29) and are depicted as functions of angular momentum in Fig. 4. A notable fact is that all moments vanish for  $\ell = 0$  or 1 because the calculated wave function becomes axially symmetric in both of the above limits. Nevertheless, the moments do not vanish for other values of the angular momentum in the interval  $0 < \ell < 1$ . Viewed from the laboratory frame, the linear momentum and mean position of the vortex read

$$\begin{aligned} \mathbf{P}_{\text{lab}} &= P(-\sin \omega t, \cos \omega t), \\ \mathbf{R}_{\text{lab}} &= R(\cos \omega t, \sin \omega t), \end{aligned} \quad (30)$$

with  $P = \omega R$ , in complete analogy with the motion of a pointlike particle rotating around the center. Therefore, generic behavior prevails in the presence of some anharmonicity ( $\lambda \neq 0$ ), whereas the stronger virial relations (19) are but a curious feature of the harmonic limit ( $\lambda = 0$ ).

In conclusion, the specific family of solutions analyzed in this paper illustrates some of the subtleties of vortex states in a confined Bose-Einstein condensate but certainly does not exhaust the possibilities. It is clear that a huge variety of multiple vortex states are possible, with increasing angular momentum, which eventually lead to a formation of regular vortex lattices. The virial theorems derived here must be satisfied in all cases and may thus be used to provide important checks of consistency, especially because they are sensitive to the presence of anharmonicity.

SK and NRC are grateful to the Kavli Institute of Theoretical Physics in Santa Barbara for hospitality and acknowledgment discussions during the “Quantum gases” program from which this work has benefited. This work was supported by EPSRC Grant Nos GR/R96026/01 (SK) and GR/S61263/01 (NRC).

[1] R.J. Donnelly, *Quantized vortices in helium II* (Cambridge University Press, 1991).  
 [2] A.L. Fetter and A.A. Svidzinsky, *J. Phys.: Condens. Matter* **13**, R135-194 (2001).  
 [3] N. Papanicolaou and T.N. Tomaras, *Nucl. Phys. B* **360**, 425 (1991).  
 [4] N. Papanicolaou and T.N. Tomaras, *Phys. Lett. A* **179**, 33 (1993).

[5] S. Komineas and N. Papanicolaou, *Nonlinearity* **11**, 265 (1998).  
 [6] G.K. Batchelor, *An introduction to fluid dynamics* (Cambridge University Press, 1967).  
 [7] P.G. Saffman, *Vortex dynamics* (Cambridge University Press, 1992).  
 [8] G.H. Derrick, *J. Math. Phys.* **5**, 1252 (1964).  
 [9] N.K. Wilkin, J.M.F. Gunn, and R.A. Smith, *Phys. Rev.*

- Lett. **80**, 2265 (1998).
- [10] D.A. Butts and D.S. Rokhsar, Nature(London) **397**, 327 (1999).
- [11] G.M. Kavoulakis, B. Mottelson, and C.J. Pethick, Phys. Rev. A **62**, 063605 (2000).
- [12] We are grateful to G.M. Kavoulakis for some explanations concerning the phase (sign) conventions associated with the coefficients  $c_m$  calculated in Ref. [11].
- [13] O.K. Vorov, P. Van Isacker, M.S. Hussein, S. Yu. Kun, and K. Bartschat, AIP conference proceedings, **777**, 72 (2005).
- [14] Y. Castin and R. Dum, Eur. Phys. J. D **7**, 399 (1999).
- [15] B.P. Anderson, P.J. Haljan, C.E. Wieman, and E.A. Cornell, Phys. Rev. Lett. **85**, 2857 (2000).
- [16] S. Komineas, N.R. Cooper, and N. Papanicolaou, e-print cond-mat/0508562.
- [17] V. Bretin, S. Stock, Y. Seurin, and J. Dalibard, Phys. Rev. Lett. **92**, 050403 (2004).